Proc. R. Soc. Lond. A. **363**, 487–502 (1978)
Printed in Great Britain

Diffraction of elastic waves by the periodic rigid boundary of a semi-infinite solid†

By J. T. Fokkema

Department of Electrical Engineering, Laboratory of Electromagnetic Research, Delft University of Technology, Delft, The Netherlands

(*Communicated by D. S. Jones, F.R.S. – Received* 23 *November* 1977)

The reflexion of an elastic wave by a rigid boundary of a semi-infinite solid with periodic profile is investigated theoretically. The problem is formulated in terms of an integral equation for the traction at a single spatial period of the boundary surface. Numerical results pertaining to the reflexion of either an incident P-wave or an incident SV-wave for a sinusoidal profile are presented. The calculations have been carried out for three different heights of the periodic profile and for two Poisson ratios (those of fused quartz and silver).

1. Introduction

In this paper the reflexion of elastic waves by a rigid boundary with a periodic profile has been investigated theoretically. Up to now most of the interest pertaining to rigid periodic boundaries has been focused on the diffraction of acoustic waves in a fluid (cf. Fortuin 1970). However, the diffraction of elastic waves is more complicated. A successful tool for the solution of elastodynamic diffraction problems is furnished by the integral-equation formalism based upon the elastodynamic representation theorem (see De Hoop 1958; Kupradze 1963; Tan 1975). By applying this technique to periodic boundaries, Fokkema & Van den Berg (1977) have solved the problem of elastodynamic diffraction by a periodic stress-free boundary. Their results show remarkable variations in the intensity curves for the reflected wave of zero spectral order at those angles of incidence where a Rayleigh wave could propagate along a plane stress-free boundary. This phenomenon has motivated a study as to what would happen with a rigid periodic boundary, since along the plane rigid boundary no surface waves can travel. In the present paper, application of the integral-equation technique leads to a vectorial integral equation for the unknown traction at a single spatial period of the boundary surface. Once the traction has been determined, the reflexion factors of waves of different reflected spectral orders can be determined. A collection of numerical results is presented pertaining to: an incident P-wave and an incident SV-wave; three different heights of the periodic profile; two Poisson ratios.

† The research reported in this paper has been supported by the Netherlands organization for the advancement of pure research (Z.W.O.).

To locate a point in space, we use the Cartesian coordinates x_1, x_2 and x_3. It is assumed that the configuration is independent of x_3. The subscript notation for vectors and tensors will be used. Latin subscripts are to be assigned the values 1, 2 and 3, while Greek subscripts are to be assigned the values 1 and 2; for repeated lower-case subscripts the summation convention holds. Occasionally, the bold-face notation will be used to denote a two-dimensional vector; in particular $\boldsymbol{x} = (x_1, x_2)$ will denote the two-dimensional position vector.

We assume that all field quantities vary sinusoidally in time with circular frequency ω. The complex time factor $\exp(-i\omega t)$ (i is the imaginary unit, t is time) is omitted throughout.

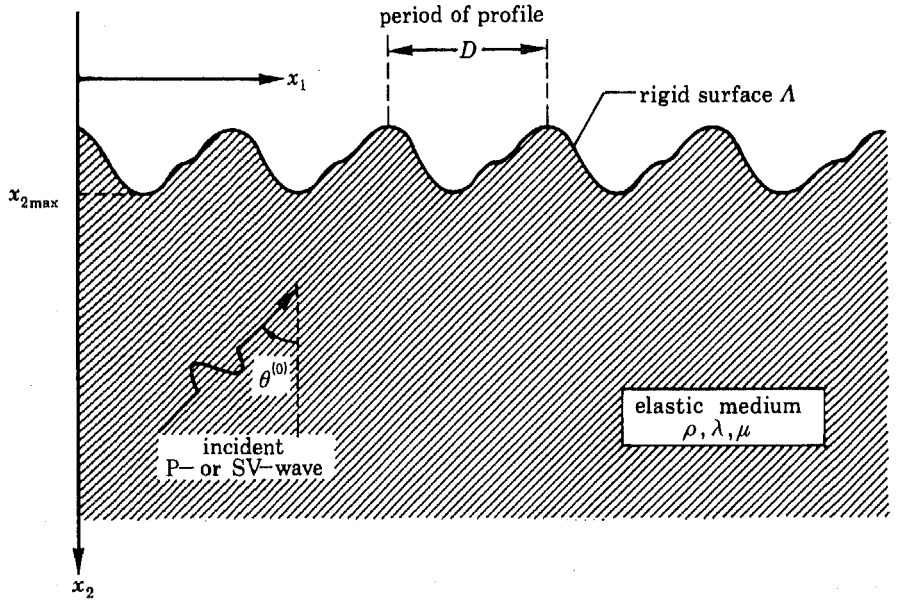

FIGURE 1. Semi-infinite elastic medium with periodic boundary and orientation of the incident wave.

2. FORMULATION OF THE PROBLEM AND METHOD OF SOLUTION

A homogeneous isotropic perfectly elastic solid occupies a semi-infinite domain with a spatially periodic rigid boundary Λ (figure 1). The mechanical properties of the material are characterized by its mass density ρ and its stiffness coefficients (see Achenbach 1973, p. 53)

$$c_{ijkl} = \lambda\delta_{ij}\delta_{kl} + \mu(\delta_{ik}\delta_{jl} + \delta_{il}\delta_{jk}), \tag{2.1}$$

in which λ and μ are the Lamé coefficients of the material and δ_{ij} is the symmetrical unit tensor of rank two: $\delta_{11} = \delta_{22} = \delta_{33} = 1$, $\delta_{ij} = 0$ if $i \neq j$.

In the medium, a two-dimensional elastic wave motion is present, of which the

particle displacement $u_\alpha = u_\alpha(\boldsymbol{x})$ and the stress $\tau_{\alpha\beta} = \tau_{\alpha\beta}(\boldsymbol{x})$ satisfy the linearized equation of motion (see Achenbach 1973, p. 51),

$$\partial_\beta \tau_{\alpha\beta} + \rho\omega^2 u_\alpha = 0, \tag{2.2}$$

and the linearized constitutive relation (see Achenbach 1973, p. 52),

$$\tau_{\alpha\beta} = c_{\alpha\beta\xi\eta}\,\partial_\xi u_\eta, \tag{2.3}$$

where ∂_β denotes the partial derivative with respect to x_β. It is convenient to introduce two-dimensional plane waves, which we distinguish as compressional waves (P-waves) and vertically polarized shear waves (SV-waves). The different quantities associated with the two types of waves are listed in table 1. In table 1, $\epsilon_{\alpha\gamma}$ denotes the anti-symmetrical unit tensor of rank two: $\epsilon_{11} = \epsilon_{22} = 0$, $\epsilon_{12} = -\epsilon_{21} = 1$.

TABLE 1. QUANTITIES ASSOCIATED WITH PLANE P- AND SV-WAVES

quantity	P-wave	SV-wave
wavenumber	$k_\mathrm{P} = \omega/c_\mathrm{P}$	$k_\mathrm{S} = \omega/c_\mathrm{S}$
wave speed	$c_\mathrm{P} = \{(\lambda+2\mu)/\rho\}^{\frac{1}{2}}$	$c_\mathrm{S} = (\mu/\rho)^{\frac{1}{2}}$
wavevector	$\boldsymbol{k}_\mathrm{P} = (k_{\mathrm{P},1}, k_{\mathrm{P},2})$	$\boldsymbol{k}_\mathrm{S} = (k_{\mathrm{S},1}, k_{\mathrm{S},2})$
particle displacement	$u_{\mathrm{P},\alpha}(\boldsymbol{x}, \boldsymbol{k}_\mathrm{P})$	$u_{\mathrm{S},\alpha}(\boldsymbol{x}, \boldsymbol{k}_\mathrm{S})$
	$= k_{\mathrm{P},\alpha}\, k_\mathrm{P}^{-1} \exp(\mathrm{i}\boldsymbol{k}_\mathrm{P}\cdot\boldsymbol{x})$	$= \epsilon_{\alpha\gamma}\, k_{\mathrm{S},\gamma}\, k_\mathrm{S}^{-1} \exp(\mathrm{i}\boldsymbol{k}_\mathrm{S}\cdot\boldsymbol{x})$
stress	$\tau_{\mathrm{P},\alpha\beta}(\boldsymbol{x}, \boldsymbol{k}_\mathrm{P})$	$\tau_{\mathrm{S},\alpha\beta}(\boldsymbol{x}, \boldsymbol{k}_\mathrm{S})$
	$= \mathrm{i}(\lambda k_{\mathrm{P},\gamma}\, k_{\mathrm{P},\gamma}\, \delta_{\alpha\beta} + 2\mu k_{\mathrm{P},\alpha}\, k_{\mathrm{P},\beta})\, k_\mathrm{P}^{-1}$	$= \mathrm{i}\mu(k_{\mathrm{S}\,\alpha}\, \epsilon_{\beta\gamma}\, k_{\mathrm{S},\gamma} + k_{\mathrm{S},\beta}\, \epsilon_{\alpha\gamma}\, k_{\mathrm{S},\gamma})\, k_\mathrm{S}^{-1}$
	$\times \exp(\mathrm{i}\boldsymbol{k}_\mathrm{P}\cdot\boldsymbol{x})$	$\times \exp(\mathrm{i}\boldsymbol{k}_\mathrm{S}\cdot\boldsymbol{x})$

TABLE 2. QUANTITIES ASSOCIATED WITH THE INCIDENT PLANE WAVE

quantity	incident P-wave	incident SV-wave
wavevector	$\boldsymbol{k}_\mathrm{P}^\mathrm{i} = (k_\mathrm{P}\sin\theta_\mathrm{P}^{(0)}, -k_\mathrm{P}\cos\theta_\mathrm{P}^{(0)})$	$\boldsymbol{k}_\mathrm{S}^\mathrm{i} = (k_\mathrm{S}\sin\theta_\mathrm{S}^{(0)}, -k_\mathrm{S}\cos\theta_\mathrm{S}^{(0)})$
intensity	$\frac{1}{2}\omega^2\rho c_\mathrm{P}$	$\frac{1}{2}\omega^2\rho c_\mathrm{S}$

The particle displacement and the stress of a plane wave propagating in the (x_1, x_2)-plane, incident upon the boundary Λ of the elastic medium, are written as

$$u_\alpha^\mathrm{i} = u_{\mathrm{P},\alpha}(\boldsymbol{x}, \boldsymbol{k}_\mathrm{P}^\mathrm{i}),$$
$$\tau_{\alpha\beta}^\mathrm{i} = \tau_{\mathrm{P},\alpha\beta}(\boldsymbol{x}, \boldsymbol{k}_\mathrm{P}^\mathrm{i}) \tag{2.4}$$

for an incident P-wave, or

$$u_\alpha^\mathrm{i} = u_{\mathrm{S},\alpha}(\boldsymbol{x}, \boldsymbol{k}_\mathrm{S}^\mathrm{i}),$$
$$\tau_{\alpha\beta}^\mathrm{i} = \tau_{\mathrm{S},\alpha\beta}(\boldsymbol{x}, \boldsymbol{k}_\mathrm{S}^\mathrm{i}) \tag{2.5}$$

for an incident SV-wave. The corresponding wavevectors and intensities are listed in table 2.

The elastodynamic quantities of the reflected field are introduced as

$$u_\alpha^\mathrm{r} = u_\alpha - u_\alpha^\mathrm{i}, \quad \tau_{\alpha\beta}^\mathrm{r} = \tau_{\alpha\beta} - \tau_{\alpha\beta}^\mathrm{i}, \tag{2.6}$$

in which, upon approaching the rigid surface, the total particle displacement has to satisfy the boundary condition,

$$u_\alpha = 0 \quad \text{on} \quad \Lambda. \tag{2.7}$$

The periodicity of the boundary surface A (with period D) and the structure of the incident wave entail a quasi-periodicity in the reflected elastodynamic field, so that $\exp(-ik_1x_1)u^{\mathrm{r}}_\alpha$ and $\exp(-ik_1x_1)\tau^{\mathrm{r}}_{\alpha\beta}$ are periodic in x_1. In the domain $x_{2\max} < x_2 < \infty$, where $x_{2\max}$ denotes the maximum value that x_2 can attain on the boundary surface A, the reflected elastodynamic field can be written as a superposition of plane waves (both P- and SV-waves) that are either propagating or exponentially decaying in the direction of increasing x_2. Let us write the corresponding representation as

$$u^{\mathrm{r}}_\alpha(\boldsymbol{x}) = \sum_{m=-\infty}^{\infty} R^{(m)}_{\mathrm{P}} u_{\mathrm{P},\alpha}(\boldsymbol{x}, \boldsymbol{k}^{(m)}_{\mathrm{P}}) + \sum_{m=-\infty}^{\infty} R^{(m)}_{\mathrm{S}} u_{\mathrm{S},\alpha}(\boldsymbol{x}, \boldsymbol{k}^{(m)}_{\mathrm{S}}) \quad (x_{2\max} < x_2 < \infty), \tag{2.8}$$

where
$$k^{(m)}_{\mathrm{P},1} = k^{(m)}_{\mathrm{S},1} = k^{(m)}_1 = k^{\mathrm{i}}_1 + 2\pi m/D,$$
$$k^{(m)}_{\mathrm{P},2} = (k^2_{\mathrm{P}} - k^{(m)2}_1)^{\frac{1}{2}}, \quad k^{(m)}_{\mathrm{S},2} = (k^2_{\mathrm{S}} - k^{(m)2}_1)^{\frac{1}{2}},$$

with
$$\mathrm{Re}\{k^{(m)}_{\mathrm{P},2}, k^{(m)}_{\mathrm{S},2}\} \geqslant 0 \quad \text{and} \quad \mathrm{Im}\{k^{(m)}_{\mathrm{P},2}, k^{(m)}_{\mathrm{S},2}\} \geqslant 0;$$

m is the spectral order. For the propagating P- and SV-waves the wavevectors $\boldsymbol{k}^{(m)}_{\mathrm{P}}$ and $\boldsymbol{k}^{(m)}_{\mathrm{S}}$ are real. They are finite in number and for them angles of reflexion can be defined, being the angles included between the x_2-axis and the direction of propagation of the wave (see table 3 and figure 2).

TABLE 3. QUANTITIES ASSOCIATED WITH A PROPAGATING REFLECTED WAVE OF SPECTRAL ORDER m

quantity	reflected P-wave	reflected SV-wave
wavevector	$\boldsymbol{k}^{(m)}_{\mathrm{P}} = (k_{\mathrm{P}} \sin\theta^{(m)}_{\mathrm{P}}, k_{\mathrm{P}} \cos\theta^{(m)}_{\mathrm{P}})$	$\boldsymbol{k}^{(m)}_{\mathrm{S}} = (k_{\mathrm{S}} \sin\theta^{(m)}_{\mathrm{S}}, k_{\mathrm{S}} \cos\theta^{(m)}_{\mathrm{S}})$
intensity	$\frac{1}{2}\omega^2\rho c_{\mathrm{P}}\lvert R^{(m)}_{\mathrm{P}}\rvert^2$	$\frac{1}{2}\omega^2\rho c_{\mathrm{S}}\lvert R^{(m)}_{\mathrm{S}}\rvert^2$
grating formula	$\sin\theta^{(m)}_{\mathrm{P}} = \sin\theta^{(0)}_{\mathrm{P}} + 2\pi m/k_{\mathrm{P}} D$	$\sin\theta^{(m)}_{\mathrm{S}} = \sin\theta^{(0)}_{\mathrm{S}} + 2\pi m/k_{\mathrm{S}} D$
Snell's law	$k_{\mathrm{P}} \sin\theta^{(0)}_{\mathrm{P}} = k_{\mathrm{S}} \sin\theta^{(0)}_{\mathrm{S}}$	

Our principal aim is to calculate the reflexion factors $R^{(m)}_{\mathrm{P}}$ and $R^{(m)}_{\mathrm{S}}$. They follow from a suitable integral representation for u^{r}_α. The latter is obtained from the two-dimensional form of the elastodynamic representation theorem applied to the domain S_1 (see figure 3) and the reflected field u^{r}_α, followed by an application to the domain S_2 and the incident field u^{i}_α (cf. Fokkema & Van den Berg 1977).

By using (2.6), the procedure leads to

$$\int_L [u^{\mathrm{g}}_{\gamma\alpha}(\boldsymbol{x}; \boldsymbol{x}')\tau_{\alpha\beta}(\boldsymbol{x}') - u_\alpha(\boldsymbol{x}')\tau^{\mathrm{g}}_{\gamma\alpha\beta}(\boldsymbol{x}; \boldsymbol{x}')]n_\beta(\boldsymbol{x}')\,\mathrm{d}s(\boldsymbol{x}')$$
$$= \{-u^{\mathrm{i}}_\gamma(\boldsymbol{x}), \tfrac{1}{2}u_\gamma(\boldsymbol{x}) - u^{\mathrm{i}}_\gamma(\boldsymbol{x}), u^{\mathrm{r}}_\gamma(\boldsymbol{x})\} \tag{2.9}$$

with
$$\boldsymbol{x} \in \{S_2, L, S_1\},$$

where n_β denotes the unit vector along the normal to L as shown in figure 3, and L corresponds with a single period of the boundary surface. If $\boldsymbol{x} \in L$ the Cauchy principal value of the relevant integral has to be understood. $u^g_{\gamma\alpha}$ and $\tau^g_{\gamma\alpha\beta}$ are the

Green tensors for the particle displacement and the stress respectively, as introduced by Fokkema & van den Berg (1977). They are given by

$$\left.\begin{aligned} u^{\mathrm{g}}_{\gamma\alpha} &= (1/\rho\omega^2)\,[\partial'_\gamma\partial'_\alpha(G_{\mathrm{S}}-G_{\mathrm{P}})+\delta_{\gamma\alpha}k_{\mathrm{S}}^2 G_{\mathrm{S}}],\\ \tau^{\mathrm{g}}_{\gamma\alpha\beta} &= c_{\alpha\beta\xi\eta}\,\partial'_\xi u^{\mathrm{g}}_{\gamma\eta},\\ \text{with}\qquad G_{\mathrm{P}} &= \sum_{m=-\infty}^{\infty}\frac{\mathrm{i}}{2k^{(m)}_{\mathrm{P},2}D}\exp\{\mathrm{i}k_1^{(m)}(x-x'_1)+\mathrm{i}k^{(m)}_{\mathrm{P},2}|x_2-x'_2|\},\\ G_{\mathrm{S}} &= \sum_{m=-\infty}^{\infty}\frac{\mathrm{i}}{2k^{(m)}_{\mathrm{S},2}D}\exp\{\mathrm{i}k_1^{(m)}(x-x'_1)+\mathrm{i}k^{(m)}_{\mathrm{S},2}|x_2-x'_2|\}, \end{aligned}\right\} \tag{2.10}$$

where ∂'_α denotes the partial derivative with respect to x'_α. The Green tensor represents the elastodynamic field generated by a phased array of line forces a period D apart, whose phases counterbalance the phase shift due to the quasi-periodicity

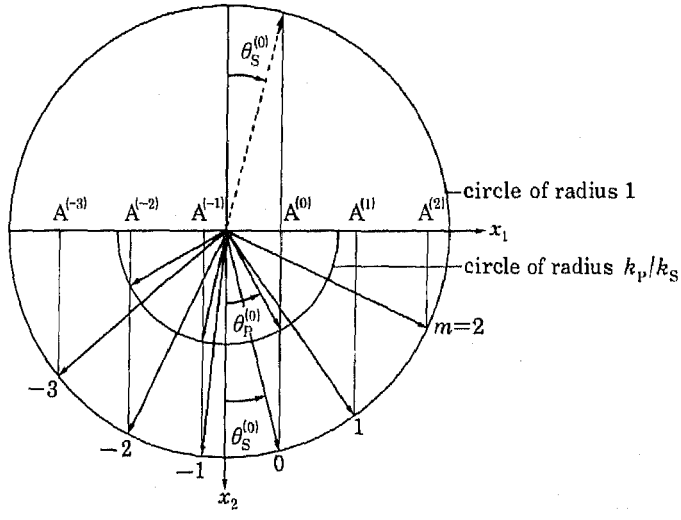

FIGURE 2. The geometrical construction of the directions of reflexion of the reflected waves of the different spectral orders from the grating formula and Snell's law, for an incident SV-wave. $\overline{\mathrm{A}^{(-3)}\mathrm{A}^{(-2)}} = \overline{\mathrm{A}^{(-2)}\mathrm{A}^{(-1)}} = \overline{\mathrm{A}^{(-1)}\mathrm{A}^{(0)}} = \overline{\mathrm{A}^{(0)}\mathrm{A}^{(1)}} = \overline{\mathrm{A}^{(1)}\mathrm{A}^{(2)}} = 2\pi/k_{\mathrm{S}}D$.

of the elastodynamic field in the configuration. Taking $\boldsymbol{x}\in S_1$ in (2.9), applying the boundary condition (2.7), and noting that $u^{\mathrm{g}}_{\gamma\alpha}$ consists of a superposition of P- and SV-waves, we obtain the following expressions for the reflexion factors $R_{\mathrm{P}}^{(m)}$ and $R_{\mathrm{S}}^{(m)}$:

$$\left.\begin{aligned} R_{\mathrm{P}}^{(m)} &= \frac{-\mathrm{i}k_{\mathrm{P}}^2}{2\rho\omega^2 k^{(m)}_{\mathrm{P},2}D}\int_L \tau_{\alpha\beta}(\boldsymbol{x}')\,n_\beta(\boldsymbol{x}')\,u_{\mathrm{P},\alpha}(\boldsymbol{x}',-\boldsymbol{k}_{\mathrm{P}}^{(m)})\,\mathrm{d}s(\boldsymbol{x}'),\\ R_{\mathrm{S}}^{(m)} &= \frac{-\mathrm{i}k_{\mathrm{S}}^2}{2\rho\omega^2 k^{(m)}_{\mathrm{S},2}D}\int_L \tau_{\alpha\beta}(\boldsymbol{x}')\,n_\beta(\boldsymbol{x}')\,u_{\mathrm{S},\alpha}(\boldsymbol{x}',-\boldsymbol{k}_{\mathrm{S}}^{(m)})\,\mathrm{d}s(\boldsymbol{x}'), \end{aligned}\right\} \tag{2.11}$$

where $u_{\mathrm{P},\alpha}$ and $u_{\mathrm{S},\alpha}$ are as given in table 1. The representations (2.11) show that $R_{\mathrm{P}}^{(m)}$ and $R_{\mathrm{S}}^{(m)}$ can be calculated as soon as the traction $\tau_{\alpha\beta}n_\beta$ on L is known. This, as

yet unknown, vector function is determined from the vectorial integral equation of the first kind

$$\int_L u^g_{\gamma\alpha}(x; x')\,\tau_{\alpha\beta}(x')\,n_\beta(x')\,ds(x') = -u^i_\gamma(x), \quad x \in L, \tag{2.12}$$

which follows by taking $x \in L$ in (2.9) and by using the boundary condition (2.7). For several reasons it is advantageous to derive a different integral equation. This is done by operating with $c_{\zeta\eta\xi\gamma}\partial_\xi$ on (2.9) with $x \in S_1$, multiplying through by

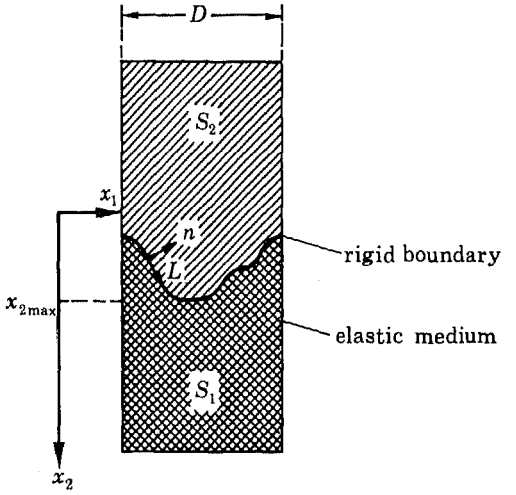

FIGURE 3. Domains to which the two-dimensional elastodynamic representation theorems are applied.

$n_\eta(x_Q)$ with $x_Q \in L$ and taking the limit $x \to x_Q$. With the aid of the relations $u^g_{\gamma\alpha}(x; x') = u^g_{\alpha\gamma}(x; x')$ and $\partial_\xi u^g_{\gamma\alpha}(x; x') = -\partial'_\xi u^g_{\gamma\alpha}(x; x')$, which can easily be established from (2.10), the result is rearranged. Then, by using the boundary condition (2.7) we obtain

$$\tfrac{1}{2}\tau_{\zeta\eta}(x)\,n_\eta(x) + \int_L \tau_{\alpha\beta}(x')\,n_\beta(x')\,\tau^g_{\alpha\zeta\eta}(x; x')\,n_\eta(x)\,ds(x') = \tau^i_{\zeta\eta}(x)\,n_\eta(x), \quad x \in L, \tag{2.13}$$

in which the Cauchy principal value of the integral has to be understood. Equation (2.13) is a vectorial integral equation of the second kind, from which the traction $\tau_{\alpha\beta}n_\beta$ on a single period L of the boundary surface can be computed. The latter integral equation seems to be new in elastodynamic diffraction theory. We prefer to base our computations on the integral equation (2.13) but shall also use the results from the integral equation (2.12) for comparison.

3. Numerical results

So far, the method presented in § 2 applies to the elastodynamic diffraction by a periodic boundary of arbitrary profile. In the present section we present the results from computations that have been performed for the sinusoidal boundary $x_2 = \frac{1}{2}h \sin(2\pi x_1/D)$ in which h is the distance from peak to trough (figure 4). For this type of boundary, a numerical solution of the integral equation based upon the method of cubic-spline approximation combined with point matching is chosen (see, for example, van den Berg 1971; Ahlberg, Nilson & Walsh 1967). In this method the interval of integration is subdivided into a number of subintervals. The unknown components of the traction are each approximated by a periodic cubic spline (i.e. a polynomial of the third degree on each subinterval, while the spline is continuous together with its first- and second-order derivatives across the mesh points of the integration interval). As a result, the integral equation is replaced by a system of linear algebraic equations. The integrals in the relevant matrix elements are computed by using the trapezoidal rule with two integration points between two successive mesh points of the chosen cubic-spline approximation. The series representations of the Green tensors $u^{\mathrm{g}}_{\gamma\alpha}$ and $\tau^{\mathrm{g}}_{\alpha\xi\eta}$ are truncated, in combination with a technique for accelerating the convergence.

As a first test of the results we check the degree of accuracy of the power relation

$$\underset{\substack{\text{propagating}\\ \text{P-waves}}}{\sum} c_{\mathrm{P}}|R_{\mathrm{P}}^{(m)}|^2 \cos\theta_{\mathrm{P}}^{(m)} + \underset{\substack{\text{propagating}\\ \text{SV-waves}}}{\sum} c_{\mathrm{S}}|R_{\mathrm{S}}^{(m)}|^2 \cos\theta_{\mathrm{S}}^{(m)} = \begin{cases} c_{\mathrm{P}} \cos\theta_{\mathrm{P}}^{(0)} \text{ for an incident P-wave,} \\ \\ c_{\mathrm{S}} \cos\theta_{\mathrm{S}}^{(0)} \text{ for an incident SV-wave.} \end{cases} \tag{3.1}$$

A second test makes use of the reciprocity relation in which we consider two different elastodynamic states distinguished by the superscripts A and B, namely $\{u_\alpha^{\mathrm{A}}, \tau_{\alpha\beta}^{\mathrm{A}}\}$ and $\{u_\alpha^{\mathrm{B}}, \tau_{\alpha\beta}^{\mathrm{B}}\}$. Each of the two states satisfies the equation of motion (2.1) and the constitutive relation (2.3). Further u_α^{A} and u_α^{B} can be written as

$$u_\alpha^{\mathrm{A}} = u_\alpha^{\mathrm{A}}(\boldsymbol{x}, \boldsymbol{k}^{\mathrm{i,A}}) + \sum_{m=-\infty}^{\infty} R_{\mathrm{P}}^{(m),\mathrm{A}} u_{\mathrm{P},\alpha}(\boldsymbol{x}, \boldsymbol{k}_{\mathrm{P}}^{(m),\mathrm{A}}) + \sum_{m=-\infty}^{\infty} R_{\mathrm{S}}^{(m),\mathrm{A}} u_{\mathrm{S},\alpha}(\boldsymbol{x}, \boldsymbol{k}_{\mathrm{S}}^{(m),\mathrm{A}}),$$

$$\text{when } x_{2\max} < x_2 < \infty,$$

and

$$u_\alpha^{\mathrm{B}} = u_\alpha^{\mathrm{B}}(\boldsymbol{x}, \boldsymbol{k}^{\mathrm{i,B}}) + \sum_{m=-\infty}^{\infty} R_{\mathrm{P}}^{(m),\mathrm{B}} u_{\mathrm{P},\alpha}(\boldsymbol{x}, \boldsymbol{k}_{\mathrm{P}}^{(m),\mathrm{B}}) + \sum_{m=-\infty}^{\infty} R_{\mathrm{S}}^{(m),\mathrm{B}} u_{\mathrm{S},\alpha}(\boldsymbol{x}, \boldsymbol{k}_{\mathrm{S}}^{(m),\mathrm{B}}),$$

$$\text{when } x_{2\max} < x_2 < \infty, \tag{3.2}$$

with $$k_1^{\mathrm{i,B}} = -k_1^{\mathrm{i,A}} - 2\pi m/D \quad (m = 0, \pm 1, \pm 2, \ldots).$$

State B refers to an incident wave with a direction of propagation opposite to one of the reflected waves of spectral order m of state A. A reciprocity relation is

furnished by application of the elastodynamic reciprocity theorem to the two elastodynamic states $\{u_\alpha^A, \tau_{\alpha\beta}^A\}$ and $\{u_\alpha^B, \tau_{\alpha\beta}^B\}$, and to the domain S_1. The reciprocity relations for propagating waves are listed in table 4 and will serve as a second test of the accuracy of the computations.

The numerical results are presented for two different materials, namely fused quartz with a Poisson ratio $\nu = 0.19$, and silver with a Poisson ratio $\nu = 0.38$. For each of them, three different values of h/D are investigated, namely $h/D = 0.1$, 0.3 and 0.5, for both an incident P-wave and an incident SV-wave. In the figures 4, 5, 6 and 7 the normalized intensities in the x_2-direction of the waves of zero spectral

TABLE 4. RECIPROCITY RELATIONS FOR PROPAGATING WAVES

state A	state B	reciprocity relation
incident SV-wave	incident P-wave	$c_P R_P^{(m),A} \cos\theta_P^{(m),A} = c_S R_S^{(m),B} \cos\theta_S^{(m),B}$
incident P-wave	incident P-wave	$R_P^{(m),A} \cos\theta_P^{(m),A} = R_P^{(m),B} \cos\theta_P^{(m),B}$
incident SV-wave	incident SV-wave	$R_S^{(m),A} \cos\theta_S^{(m),A} = R_S^{(m),B} \cos\theta_S^{(m),B}$

order $I_P^{(0)}$ and $I_S^{(0)}$ are plotted as a function of the angle of incidence. The normalized intensity in the x_2-direction of the wave of spectral order m is obtained by dividing the intensity of the reflected field of spectral order m in the x_2-direction by the intensity of the incident field in the x_2-direction. Hence

$$\left.\begin{aligned} I_P^{(m)} &= \frac{\cos\theta_P^{(m)}}{\cos\theta_P^{(0)}} |R_P^{(m)}|^2, \\ I_S^{(m)} &= \frac{c_S}{c_P} \frac{\cos\theta_S^{(m)}}{\cos\theta_P^{(0)}} |R_S^{(m)}|^2, \end{aligned}\right\} \quad \text{for an incident P-wave,} \tag{3.3}$$

and

$$\left.\begin{aligned} I_S^{(m)} &= \frac{\cos\theta_S^{(m)}}{\cos\theta_S^{(0)}} |R_S^{(m)}|^2, \\ I_P^{(m)} &= \frac{c_P}{c_S} \frac{\cos\theta_P^{(m)}}{\cos\theta_S^{(0)}} |R_P^{(m)}|^2, \end{aligned}\right\} \quad \text{for an incident SV-wave.} \tag{3.4}$$

Figures 4 and 6 show the results pertaining to $\nu = 0.19$ ($k_S D = 6$ with $k_P D = 3.71$; and $k_S D = 9$ with $k_P D = 5.57$) for an incident P-wave and an incident SV-wave, respectively.

Figures 5 and 7 show the results pertaining to $\nu = 0.38$ ($k_S D = 6$ with $k_P D = 2.64$; and $k_S D = 9$ with $k_P D = 3.96$) for an incident P-wave and an incident SV-wave, respectively.

From the figures we conclude that fluctuations in the intensity curves only appear when a reflected wave of spectral order m changes its character from propagating to evanescent or vice versa. This effect is more pronounced the deeper the grooves are. For reference, the corresponding angles of incidence are listed in tables 5 and 6 (for $\nu = 0.19$ and $\nu = 0.38$ respectively).

Further, we notice that the intensity curves of $I_S^{(0)}$ in figure 4 and the intensity curves of $I_P^{(0)}$ in figure 6 are of the same shape, but on a different scale; and similarly

for $I_S^{(0)}$ in figure 5 and $I_P^{(0)}$ in figure 7. This also directly follows from the first reciprocity relation of table 4 in conjunction with the symmetry of the profile. For completeness, we have also calculated the intensities of the reflected waves by a plane rigid boundary for $\nu = 0.19$ and $\nu = 0.38$ with the aid of the formulas given in Achenbach (1973, p. 177). The latter curves nearly coincide with the results for $h/D = 0.1$, so that we did not present these curves in the figures.

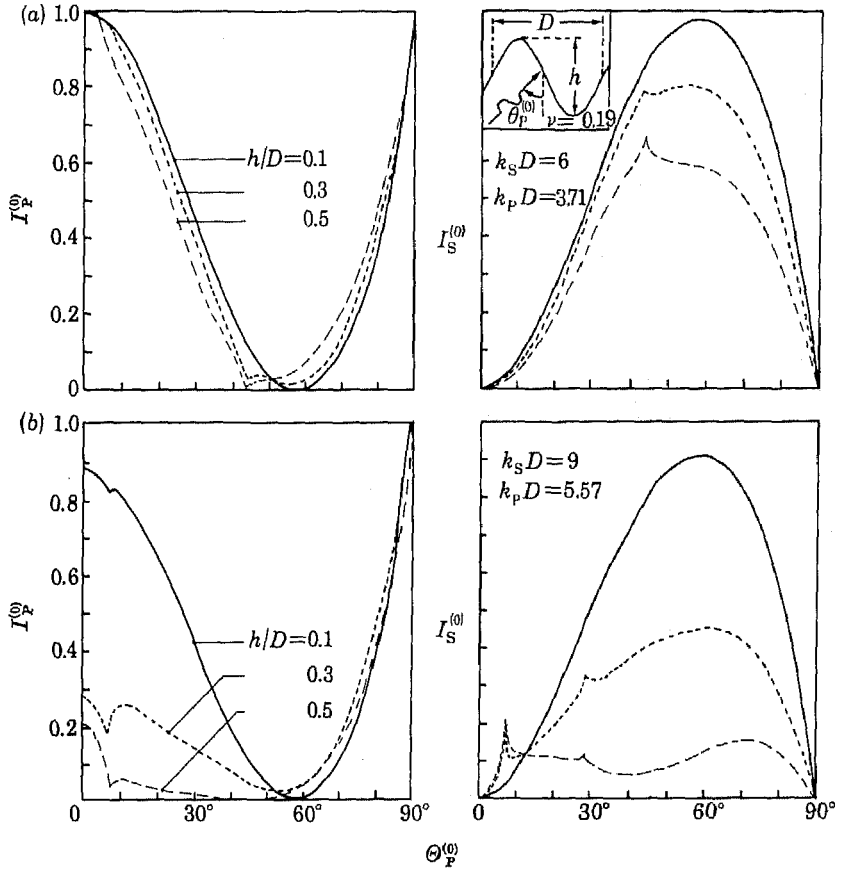

FIGURE 4. The normalized intensities in the x_3-direction $I_P^{(0)}$ and $I_S^{(0)}$ of the zero spectral order (see (3.3)) as a function of the angle of incidence $\theta_P^{(0)}$ for a sinusoidal profile. (Poisson ratio $\nu = 0.19$, incident P-wave; (*a*) $k_S D = 6$, (*b*) $k_S D = 9$.)

The computations have been performed on the IBM 370/158 computer of the Computing Centre of the Delft University of Technology. The computing time to calculate the quantities $I_P^{(0)}$ and $I_S^{(0)}$ for a single value of the angle of incidence is 8, 14 and 19 s for $h/D = 0.1$, 0.3 and 0.5, respectively when $k_S D = 9$. In the computations we have used a combination of single (six digits) and double (16 digits) precision. We have used a fully double-precision program to investigate whether the round-off errors are significant. It turned out that the error originates from the

numerical discretization of the integral equation, the numerical evaluation of the integrals in the matrix elements, and the truncation of the series representation of the Green tensor. An estimate of these errors has been made by increasing the number of linear equations that approximate the integral equation, the number of integration points to evaluate the integrals in the matrix elements, and the number of terms to represent the Green tensor. We then estimated that our results presented in the figures 4, 5, 6 and 7 have an absolute error always less than 0.005.

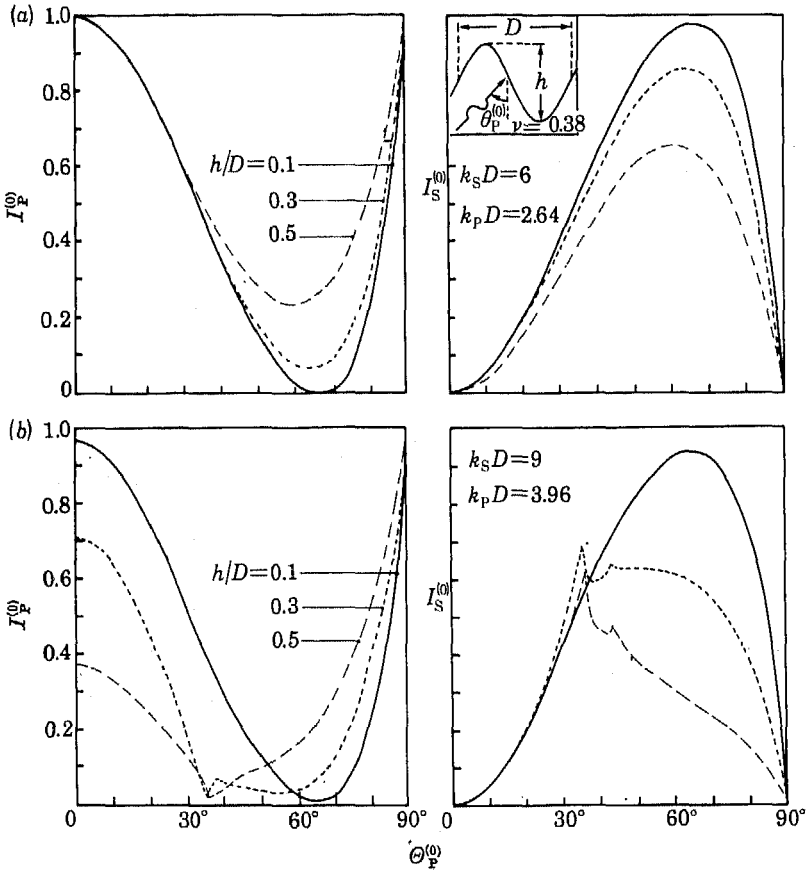

FIGURE 5. The normalized intensities in the x_3-direction $I_P^{(0)}$ and $I_S^{(0)}$ of the zero spectral order (see (3.3)) as a function of the angle of incidence $\theta_P^{(0)}$ for a sinusoidal profile. (Poisson ratio $\nu = 0.38$, incident P-wave: (a) $k_S D = 6$, (b) $k_S D = 9$.)

In tables 7 and 8 the results obtained by the method based on the integral equation of the second kind (2.13) are compared with the results by the method based on the integral equation of the first kind (2.12) for a P-wave, incident upon the boundary at an angle $\theta_P^{(0)} = 45°$; $h/D = 0.1, 0.3$ and 0.5; $k_S D = 6$ with $k_P D = 3.71$ and $k_S D = 9$ with $k_P D = 5.57$, respectively ($\nu = 0.19$). In these tables M is the total number of equations and $2K+1$ is the number of terms to represent the Green tensor.

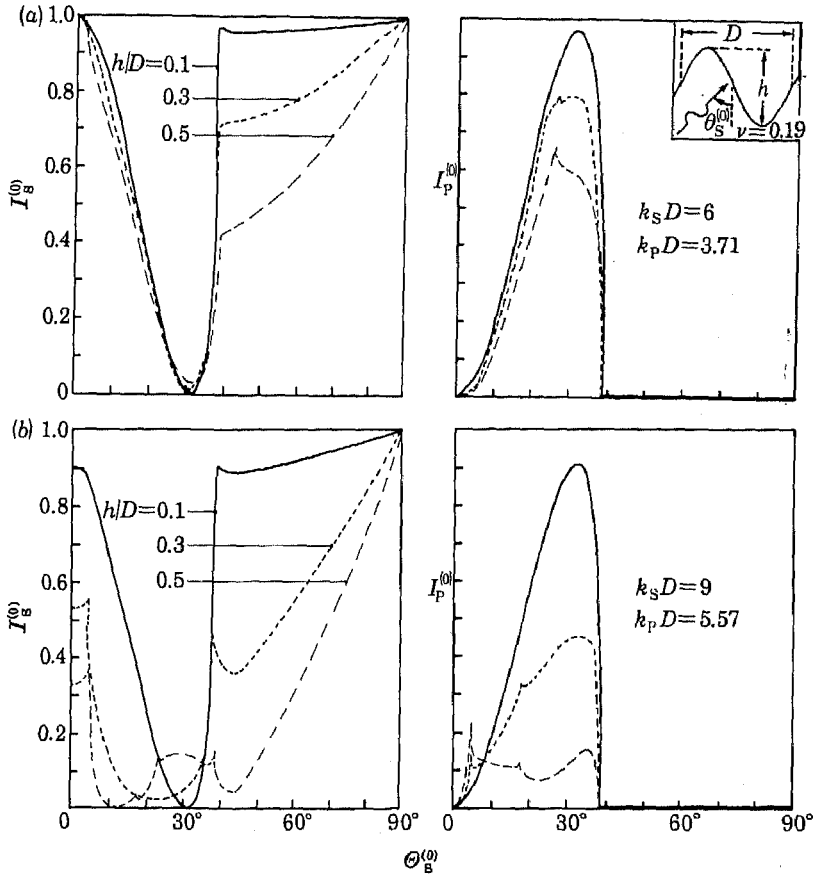

FIGURE 6. The normalized intensities in the x_2-direction $I_R^{(0)}$ and $I_P^{(0)}$ of the zero spectral order (see (3.4)) as a function of the angle of incidence $\theta_R^{(0)}$ for a sinusoidal profile. (Poisson ratio $\nu = 0.19$, incident SV-wave: (*a*) $k_S D = 6$, (*b*) $k_S D = 9$.)

TABLE 5. THE INTERVALS OF THE ANGLES OF INCIDENCE (IN DEGREES), IN WHICH THE REFLECTED WAVE OF SPECTRAL ORDER m IS PROPAGATING, FOR A POISSON RATIO $\nu = 0.19$

The angle of incidence varies between 0 and 90°.

	$k_S D = 6$, $k_P D = 3.71$				$k_S D = 9$, $k_P D = 5.57$			
spectral order	inc. P		inc. SV		inc. P		inc. SV	
m	refl. P	refl. SV	refl. SV	refl. P	refl. P	refl. SV	refl. SV	refl. P
−2	—	—	—	—	—	39.8–90	23.3–90	51–90
−1	43.8–90	4.4–90	2.7–90	25.4–90	7.4–90	0–90	0–90	4.6–90
0	0–90	0–90	0–90	0–38.2	0–90	0–90	0–90	0–38.2
1	—	—	—	—	—	0–29.2	0–17.6	

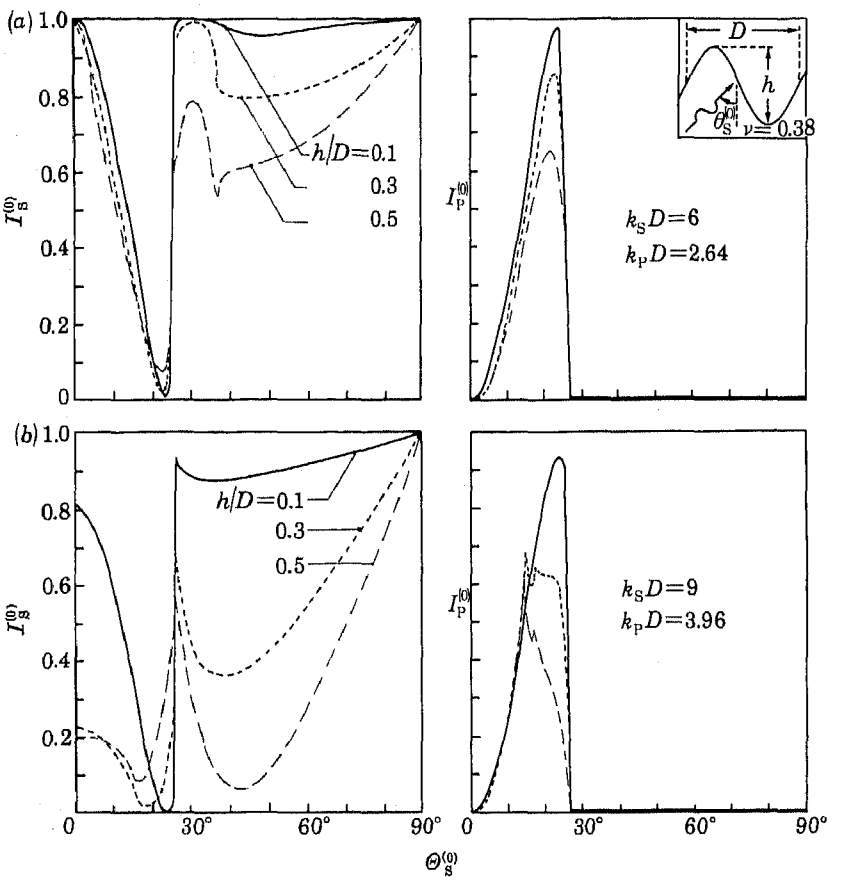

FIGURE 7. The normalized intensities in the x_2-direction $I_S^{(0)}$ and $I_P^{(0)}$ of the zero spectral order (see (3.4)) as a function of the angle of incidence $\theta_S^{(0)}$ for a sinusoidal profile. (Poisson ratio $\nu = 0.38$, incident SV-wave: (*a*) $k_S D = 6$, (*b*) $k_S D = 9$.)

TABLE 6. THE INTERVALS OF THE ANGLES OF INCIDENCE (IN DEGREES), IN WHICH THE REFLECTED WAVE OF SPECTRAL ORDER m IS PROPAGATING, FOR A POISSON RATIO $\nu = 0.38$

The angle of incidence varies between 0 and 90°.

	$k_S D = 6$, $k_P D = 2.64$				$k_S D = 9$, $k_P D = 3.96$			
	inc. P		inc. SV		inc. P		inc. SV	
spectral order m	refl. P	refl. SV	refl. SV	refl. P	refl. P	refl. SV	refl. SV	refl. P
−2	—	—	—	—	—	64.2–90	23.3–90	73–90
−1	—	6.2–90	2.7–90	37.4–90	35.9–90	0–90	0–90	15–90
0	0–90	0–90	0–90	0–26.1	0–90	0–90	0–90	0–26.1
1	—	—	—	—	—	0–43.3	0–7.6	

TABLE 7. RESULTS FOR AN INCIDENT P-WAVE WITH AN ANGLE OF INCIDENCE $\theta_P^{(0)} = 45°$, $h/D = 0.1$, 0.3 AND 0.5; $k_S D = 9$ WITH $k_P D = 5.57$ ($\nu = 0.19$)

	$h/D = 0.1$, integral equation of the		$h/D = 0.3$, integral equation of the		$h/D = 0.5$, integral equation of the	
	first kind	second kind	first kind	second kind	first kind	second kind
M	10	10	13	13	15	15
K	10	10	10	10	10	10
$I_P^{(-1)}$	0.0743	0.0744	0.4729	0.4753	0.6812	0.6836
$I_P^{(0)}$	0.1054	0.1049	0.0444	0.0419	0.0078	0.0072
$I_S^{(-2)}$	0.0001	0.0001	0.0047	0.0050	0.0130	0.0137
$I_S^{(-1)}$	0.0143	0.0142	0.0752	0.0726	0.2214	0.2172
$I_S^{(0)}$	0.8053	0.8063	0.4020	0.4049	0.0763	0.0767
$\sum_n I_P^{(n)} + \sum_m I_S^{(m)} = 1$	0.9994	0.9999	0.9992	0.9997	0.9997	0.9984

TABLE 8. RESULTS FOR AN INCIDENT P-WAVE WITH AN ANGLE OF INCIDENCE $\theta_P^{(0)} = 45°$; $h/D = 0.1$, 0.3 AND 0.5; $k_S D = 6$ WITH $k_P D = 3.71$ ($\nu = 0.19$)

	$h/D = 0.1$, integral equation of the		$h/D = 0.3$, integral equation of the		$h/D = 0.5$, integral equation of the	
	first kind	second kind	first kind	second kind	first kind	second kind
M	10	10	12	12	14	14
K	10	10	10	10	10	10
$I_P^{(-1)}$	0.0159	0.0158	0.0980	0.0980	0.1719	0.1731
$I_P^{(0)}$	0.1042	0.1040	0.0443	0.0432	0.0198	0.0184
$I_S^{(-1)}$	0.0116	0.0115	0.0874	0.0863	0.1851	0.1849
$I_S^{(0)}$	0.8679	0.8684	0.7700	0.7718	0.6231	0.6238
$\sum_n I_P^{(n)} + \sum_m I_S^{(m)} = 1$	0.9996	0.9997	0.9997	0.9993	0.9999	1.0002

The author wishes to thank Professor A. T. de Hoop and Dr P. M. van den Berg for their suggestions and remarks. The financial support of the Netherlands organization for the advancement of pure research (Z.W.O.) is gratefully acknowledged.

REFERENCES

Achenbach, J. D. 1973 *Wave propagation in elastic solids*. Amsterdam: North-Holland.

Ahlberg, J. H., Nilson, E. N. & Walsh, J. L. 1967 *The theory of splines and their applications*. New York, London: Academic Press.

van den Berg, P. M. 1971 *Appl. Sci. Res.* **24**, 261–293.

Fokkema, J. T. & van den Berg, P. M. 1977 *J. acoust. Soc. Am.* **61** (in the press).

Fortuin, L. 1970 *J. acoust. Soc. Am.* **47**, 1209–1228.

De Hoop, A. T. 1958 Representation theorems for the displacement in an elastic solid and their application to elastodynamic diffraction theory. Ph.D. dissertation. Delft: University of Technology.

Kupradze, V. D. 1963 *Progress in solid mechanics*, vol. 3 (eds I. N. Sneddon & R. Hill). Amsterdam: North-Holland.

Tan, T. H. 1975 *Appl. Sci. Res.* **31**, 29–53.

Appendix A

The starting point of the derivation of the integral representation is the two-dimensional form of the elastodynamic reciprocity relation. In this relation we are concerned with two elastodynamic states distinguished by the superscripts A and B, respectively. Both elastodynamic states are present in one and the same medium and vary sinusoidally in time with the same circular frequency ω. The equations of motion and the constitutive equations pertaining to both states can be written as

$$\left.\begin{aligned} \partial_\beta \tau_{\alpha\beta}^{\mathrm{A,B}} + \rho\omega^2 u_\alpha^{\mathrm{A,B}} &= -f_\alpha^{\mathrm{A,B}}, \\ \tau_{\alpha\beta}^{\mathrm{A,B}} &= c_{\alpha\beta\xi\eta}\,\partial_\xi u_\eta^{\mathrm{A,B}}, \end{aligned}\right\} \tag{A 1}$$

in which $f_\alpha^{\mathrm{A,B}}$ denotes the density of the body force. Let C be a simple closed contour and let S be its interior, then the elastodynamic reciprocity relation is given by

$$\oint_C [u_\alpha^{\mathrm{B}} \tau_{\alpha\beta}^{\mathrm{A}} - u_\alpha^{\mathrm{A}} \tau_{\alpha\beta}^{\mathrm{B}}]\, n_\beta(\boldsymbol{x}')\, \mathrm{d}s(\boldsymbol{x}') = \iint_S [f_\alpha^{\mathrm{B}} u_\alpha^{\mathrm{A}} - f_\alpha^{\mathrm{A}} u_\alpha^{\mathrm{B}}]\, \mathrm{d}x_1'\, \mathrm{d}x_2', \tag{A 2}$$

where n_β denotes the unit vector along the outward normal to C. In order to derive an integral representation for u_α^{r}, we associate with the state A $\{u_\alpha^{\mathrm{r}}, \tau_{\alpha\beta}^{\mathrm{r}}\}$, obeying the homogeneous differential equation $\partial_\beta \tau_{\alpha\beta}^{\mathrm{r}} + u_\alpha^{\mathrm{r}} = 0$ and the constitutive equation $\tau_{\alpha\beta}^{\mathrm{r}} = c_{\alpha\beta\xi\eta}\,\partial_\xi u_\eta^{\mathrm{r}}$. For the state B we take an auxiliary state of disturbance, the so-called Green solution $u_\alpha^{\mathrm{g}} = u_\alpha^{\mathrm{g}}(\boldsymbol{x}; \boldsymbol{x}')$ and $\tau_{\alpha\beta}^{\mathrm{g}} = \tau_{\alpha\beta}^{\mathrm{g}}(\boldsymbol{x}; \boldsymbol{x}')$, being a vector-valued displacement field and its associated tensor-valued stress field.

The equation of motion and the constitutive equation for the Green solution are

$$\partial_\beta' \tau_{\alpha\beta}^{\mathrm{g}} + \rho\omega^2 u_\alpha^{\mathrm{g}} = -b_\alpha\, \delta(\boldsymbol{x} - \boldsymbol{x}'), \quad \tau_{\alpha\beta}^{\mathrm{g}} = c_{\alpha\beta\xi\eta}\,\partial_\xi' u_\eta^{\mathrm{g}}, \tag{A 3}$$

in which $\delta(\boldsymbol{x} - \boldsymbol{x}')$ is the two-dimensional delta function and b_α an arbitrary constant vector.

For our problem we apply the reciprocity relation to a domain S_1 inside C for which we choose the closed contour consisting of two straight lines parallel to the x_2-axis, a period D apart, together with the curve L corresponding with a single period of the boundary profile and finally a straight line parallel to the x_1-axis, not intersecting L (see figure 3). Then, we obtain for a point P inside S_1

$$\oint_C [u_\alpha^{\mathrm{g}}(\boldsymbol{x}; \boldsymbol{x}')\, \tau_{\alpha\beta}^{\mathrm{r}}(\boldsymbol{x}') - u_\alpha^{\mathrm{r}}(\boldsymbol{x}')\, \tau_{\alpha\beta}^{\mathrm{g}}(\boldsymbol{x}; \boldsymbol{x}')]\, n_\beta(\boldsymbol{x}')\, \mathrm{d}s(\boldsymbol{x}') = b_\alpha\, u_\alpha^{\mathrm{r}}(\boldsymbol{x}), \quad \boldsymbol{x} \in S_1. \tag{A 4}$$

The Green solution is further chosen in such a way that in the integral representation (A 4) only the contribution from L remains. This is achieved by requiring that $u_\alpha^{\mathrm{g}}(\boldsymbol{x}; \boldsymbol{x}')$ consists of waves which travel away from the source point P with co-ordinates x_1, x_2 in the x_2'-direction. Then it can be shown that the contribution from the straight line parallel to the x_1-axis vanishes. Further, by requiring that $u_\alpha^{\mathrm{g}}(\boldsymbol{x}; \boldsymbol{x}')$ possesses, at a fixed value of x_2, a phase variation exactly opposite to the

one of u_α^{r}, the contributions from the two straight lines parallel to the x_2-axis cancel each other. An enumeration of these requirements for the Green solution yields

$$\left.\begin{aligned}
&\partial'_\beta \tau^{\mathrm{g}}_{\alpha\beta} + \rho\omega^2 u^{\mathrm{g}}_\alpha = -b_\alpha\,\delta(\boldsymbol{x}-\boldsymbol{x}'),\\
&\tau^{\mathrm{g}}_{\alpha\beta} = c_{\alpha\beta\xi\eta}\,\partial'_\xi u^{\mathrm{g}}_\eta,\\
&\exp\{\mathrm{i}k_1^{\mathrm{i}}(x'_1-x_1)\}\,u^{\mathrm{g}}_\alpha(\boldsymbol{x};\boldsymbol{x}') = \text{periodic in } (x'_1-x_1) \text{ with period } D.\\
&\text{and}\\
&u^{\mathrm{g}}_\alpha(\boldsymbol{x};\boldsymbol{x}') \text{ consists of waves which travel from } (x_1,x_2) \text{ in the } x'_2\text{-direction.}
\end{aligned}\right\} \tag{A 5}$$

Expansion in a Fourier series with period D in (x'_1-x_1) yields

$$\exp\{\mathrm{i}k_1^{\mathrm{i}}(x'_1-x_1)\}\,u^{\mathrm{g}}_\alpha(\boldsymbol{x};\boldsymbol{x}') = \sum_{n=-\infty}^{\infty} U^{\mathrm{g}(n)}_\alpha(x_2;x'_2)\exp\left\{\frac{\mathrm{i}2\pi n}{D}(x_1-x'_1)\right\} \tag{A 6}$$

or, with $k_1^{(n)} = k_1^{\mathrm{i}} + 2\pi n/D$,

$$u^{\mathrm{g}}_\alpha(\boldsymbol{x};\boldsymbol{x}') = \sum_{n=-\infty}^{\infty} U^{\mathrm{g}(n)}_\alpha(x_2;x'_2)\exp\{\mathrm{i}k_1^{(n)}(x_1-x'_1)\}. \tag{A 7}$$

Substituting (A 7) in the equation of motion and using the orthogonality of $\exp\{\mathrm{i}k_1^{(n)}(x_1-x'_1)\}$, we obtain for all n

$$\begin{bmatrix} \{\mu\partial'^2_2 - (\lambda+2\mu)\,k_1^{(n)2} + \rho\omega^2\} & -\mathrm{i}k_1^{(n)}(\lambda+\mu)\,\partial'_2 \\ -\mathrm{i}k_1^{(n)}(\lambda+\mu)\,\partial'_2 & \{(\lambda+2\mu)\,\partial'^2_1 - \mu k_1^{(n)2} + \rho\omega^2\} \end{bmatrix} \begin{bmatrix} U_1^{\mathrm{g}(n)} \\ U_2^{\mathrm{g}(n)} \end{bmatrix} = \begin{bmatrix} -b_1\,\delta(x_2-x'_2)/D \\ -b_2\,\delta(x_2-x'_2)/D \end{bmatrix}. \tag{A 8}$$

In order to obtain a solution of (A 8), we take a Fourier transform of $U^{\mathrm{g}(n)}_\alpha$ with respect to $(x_2-x'_2)$. The latter is given by

$$\tilde{U}^{\mathrm{g}(n)}_\alpha(\kappa) = \int_{-\infty}^{\infty} U^{\mathrm{g}(n)}_\alpha(x_2;x'_2)\exp\{\mathrm{i}\kappa(x_2-x'_2)\}\,\mathrm{d}(x_2-x'_2). \tag{A 9}$$

The Fourier inversion theorem then yields

$$U^{\mathrm{g}(n)}_\alpha(x_2,x'_2) = \frac{1}{2\pi}\int_{-\infty}^{\infty} \tilde{U}^{\mathrm{g}(n)}_\alpha(\kappa)\exp\{-\mathrm{i}\kappa(x_2-x'_2)\}\,\mathrm{d}\kappa. \tag{A 10}$$

Application of (A 9) to (A 8) yields

$$\begin{bmatrix} \tilde{U}_1^{\mathrm{g}(n)} \\ \tilde{U}_2^{\mathrm{g}(n)} \end{bmatrix} = \begin{bmatrix} \dfrac{k_{\mathrm{S}}^2}{S} + k_1^{(n)2}\left(\dfrac{1}{P}-\dfrac{1}{S}\right) & \kappa k_1^{(n)}\left(\dfrac{1}{S}-\dfrac{1}{P}\right) \\ \kappa k_1^{(n)}\left(\dfrac{1}{S}-\dfrac{1}{P}\right) & \dfrac{k_{\mathrm{S}}^2}{S} + \kappa^2\left(\dfrac{1}{P}-\dfrac{1}{S}\right) \end{bmatrix} \begin{bmatrix} b_1/\rho\omega^2 D \\ b_2/\rho\omega^2 D \end{bmatrix}, \tag{A 11}$$

with $P = \kappa^2 - (k_{\mathrm{P}}^2 - k_1^{(n)2})$, and $S = \kappa^2 - (k_{\mathrm{S}}^2 - k_1^{(n)2})$, in which we have used the relations $k_{\mathrm{P}}^2 = \rho\omega^2/(\lambda+2\mu)$ and $k_{\mathrm{S}}^2 = \rho\omega^2/\mu$. The Green solution is now obtained by the inverse transformation of the expression (A 11). To this end we make use of the following integral formulas:

$$\left.\begin{aligned}
&\frac{1}{2\pi}\int_{-\infty}^{\infty} \frac{\exp\{\mathrm{i}\kappa(x'_2-x_2)\}}{\kappa^2 - k_{\mathrm{P},2}^{(n)2}}\,\mathrm{d}\kappa = \frac{\mathrm{i}}{2k_{\mathrm{P},2}^{(n)}}\exp\{\mathrm{i}k_{\mathrm{P},2}^{(n)}|x_2-x'_2|\},\\
&\frac{1}{2\pi}\int_{-\infty}^{\infty} \frac{\exp\{\mathrm{i}\kappa(x'_2-x_2)\}}{\kappa^2 - k_{\mathrm{S},2}^{(n)2}}\,\mathrm{d}\kappa = \frac{\mathrm{i}}{2k_{\mathrm{S},2}^{(n)}}\exp\{\mathrm{i}k_{\mathrm{S},2}^{(n)}|x_2-x'_2|\},
\end{aligned}\right\} \tag{A 12}$$

with $$k_{\mathrm{P},2}^{(n)} = \{k_{\mathrm{P}}^2 - k_1^{(n)2}\}^{\frac{1}{2}}, \quad k_{\mathrm{S},2}^{(n)} = \{k_{\mathrm{S}}^2 - k_1^{(n)2}\}^{\frac{1}{2}},$$

and $$\mathrm{Re}\{k_{\mathrm{P},2}^{(n)}, k_{\mathrm{S},2}^{(n)}\} \geqslant 0, \quad \mathrm{Im}\{k_{\mathrm{P},2}^{(n)}, k_{\mathrm{S},2}^{(n)}\} \geqslant 0,$$

so that with this choice we have also satisfied the last requirement of (A 5). Using (A 12), together with the rule that the factor $\mathrm{i}\kappa$ in the κ-domain corresponds to ∂_2' in the $(x_2 - x_2')$-domain and noting that the factor $-\mathrm{i}k_1^{(n)}$ can be replaced by ∂_1', we finally obtain

$$u_\alpha^{\mathrm{g}} = (1/\rho\omega^2)[\partial_\alpha' \partial_\gamma'(G_{\mathrm{S}} - G_{\mathrm{P}}) + \delta_{\alpha\gamma} k_{\mathrm{S}}^2 G_{\mathrm{S}}] b_\gamma, \tag{A 13}$$

with $$G_{\mathrm{P}} = \sum_{n=-\infty}^{\infty} (\mathrm{i}/2k_{\mathrm{P},2}^{(n)} D) \exp\{\mathrm{i}k_1^{(n)}(x_1 - x_1') + \mathrm{i}k_{\mathrm{P},2}^{(n)}|x_2 - x_2'|\},$$

$$G_{\mathrm{S}} = \sum_{n=-\infty}^{\infty} (\mathrm{i}/2k_{\mathrm{S},2}^{(n)} D) \exp\{\mathrm{i}k_1^{(n)}(x_1 - x_1') + \mathrm{i}k_{\mathrm{S},2}^{(n)}|x_2 - x_2'|\}.$$

From (A 4), a representation for the particle displacement is obtained by observing that b_α is arbitrary and that the Green solution depends linearly on the components of b_α. To express this dependence, we introduce a tensor of rank two, $u_{\gamma\alpha}^{\mathrm{g}} = u_{\gamma\alpha}^{\mathrm{g}}(\boldsymbol{x}; \boldsymbol{x}')$, and a tensor of rank three, $\tau_{\gamma\alpha\beta}^{\mathrm{g}} = \tau_{\gamma\alpha\beta}^{\mathrm{g}}(\boldsymbol{x}; \boldsymbol{x}')$, which relate u_α^{g} and $\tau_{\alpha\beta}^{\mathrm{g}}$ through

$$\left.\begin{aligned} u_\alpha^{\mathrm{g}} &= b_\gamma u_{\gamma\alpha}^{\mathrm{g}}, \\ \tau_{\alpha\beta}^{\mathrm{g}} &= b_\gamma \tau_{\gamma\alpha\beta}^{\mathrm{g}}, \end{aligned}\right\} \tag{A 14}$$

so that we can write for $u_{\gamma\alpha}^{\mathrm{g}}$ and $\tau_{\gamma\alpha\beta}^{\mathrm{g}}$

$$\left.\begin{aligned} u_{\gamma\alpha}^{\mathrm{g}} &= (1/\rho\omega^2)[\partial_\gamma' \partial_\alpha'(G_{\mathrm{S}} - G_{\mathrm{P}}) + \delta_{\gamma\alpha} k_{\mathrm{S}}^2 G_{\mathrm{S}}], \\ \tau_{\gamma\alpha\beta}^{\mathrm{g}} &= c_{\alpha\beta\xi\eta} \partial_\xi' u_{\gamma\eta}^{\mathrm{g}}. \end{aligned}\right\} \tag{A 15}$$

Substituting (A 15) in (A 4) and noting that the resulting equation should hold for any choice of b_γ, we obtain

$$\int_L [u_{\gamma\alpha}^{\mathrm{g}}(\boldsymbol{x}; \boldsymbol{x}') \tau_{\alpha\beta}^{\mathrm{r}}(\boldsymbol{x}') - u_\alpha^{\mathrm{r}}(\boldsymbol{x}') \tau_{\gamma\alpha\beta}^{\mathrm{g}}(\boldsymbol{x}; \boldsymbol{x}')] n_\beta(\boldsymbol{x}')\, \mathrm{d}s(\boldsymbol{x}') = u_\gamma^{\mathrm{r}}(\boldsymbol{x}), \quad \boldsymbol{x} \in S_1. \tag{A 16}$$

Application of the reciprocity relation to the incident field u_α^{i} and the domain S_2, keeping P fixed in S_1 we obtain

$$\int_L [u_{\gamma\alpha}^{\mathrm{g}}(\boldsymbol{x}; \boldsymbol{x}') \tau_{\alpha\beta}^{\mathrm{i}}(\boldsymbol{x}') - u_\alpha^{\mathrm{i}}(\boldsymbol{x}') \tau_{\gamma\alpha\beta}^{\mathrm{g}}(\boldsymbol{x}; \boldsymbol{x}')] n_\beta(\boldsymbol{x}')\, \mathrm{d}s(\boldsymbol{x}') = 0, \quad \boldsymbol{x} \in S_1. \tag{A 17}$$

Combining (A 16) and (A 17), using (2.6) and the boundary condition (2.7), we obtain

$$u_\gamma^{\mathrm{r}}(\boldsymbol{x}) = \int_L u_{\gamma\alpha}^{\mathrm{g}}(\boldsymbol{x}; \boldsymbol{x}') \tau_{\alpha\beta}(\boldsymbol{x}') n_\beta(\boldsymbol{x}')\, \mathrm{d}s(\boldsymbol{x}'), \quad \boldsymbol{x} \in S_1. \tag{A 18}$$

The unknown traction $\tau_{\alpha\beta} n_\beta$ can be determined from the integral equation (2.12) or (2.13), obtained by choosing P on L. We observe that, for $x_2 \geqslant x_{2\max}$, $x_2 - x_2' \geqslant 0$ for all x_2'; we then arrive at the expansion (2.8) together with the expressions (2.11) for the reflexion factors. Generally, the expansion (2.8) is not allowed in the grooves for $x_2 < x_{2\max}$, however in that case (A 18) still gives the exact representation for the reflected field.